# Crossed beam studies of the $O(^3P,^1D) + CH_3I$ reactions: Direct evidence of intersystem crossing

**Michele Alagia,†[a] Nadia Balucani,[a] Laura Cartechini,[a] Piergiorgio Casavecchia,*[a] Michiel van Beek,‡[a] Gian Gualberto Volpi,[a] Laurent Bonnet,[b] and Jean Claude Rayez[b]**

[a] *Dipartimento di Chimica, Università di Perugia, Via Elce di Sotto 8, 06123 Perugia, Italy. E-mail: piero@dyn.unipg.it*

[b] *Laboratoire de Physico-Chimie Moléculaire, Université Bordeaux 1, 33405 Talence Cedex, France*

***Received 13th April 1999***

The angular and velocity distributions of the IO product from the reactions $O(^3P,^1D) + CH_3I$ have been obtained in crossed beam experiments with a rotating mass spectrometer detector at collision energies of 55.2 and 64.0 kJ $mol^{-1}$. The center of mass product angular and translational energy distributions for both the $O(^3P)$ and $O(^1D)$ reactions have been derived, and the effect of electronic excitation and the role of intersystem crossing (ISC) assessed. The $O(^3P)$ reaction proceeds, with comparable cross-section, both *via* a direct mechanism on the triplet potential energy surface with rebound dynamics and *via* a long-lived complex mechanism following ISC from the triplet to the singlet surface. The $O(^1D)$ reaction proceeds on the singlet surface *via* formation of a complex that lives about one rotational period and also, with comparable cross-section, *via* direct rebound dynamics following a nearly collinear O–I–$CH_3$ approach geometry. ISC from the triplet to the singlet surface is attributed to the presence of the heavy halogen atom and occurs for bent geometry. These findings are corroborated by recent theoretical calculations on the stationary points of the potential energy surfaces for the system. Calculations based on phase space theory, which assumes conservation of energy and angular momentum and takes into account the various degrees of freedom involved, have been performed; the product angular and translational energy distributions derived for the $O(^3P)$ reaction proceeding *via* ISC and long-lived collision complex formation are in very good agreement with the experimental quantities.

## I. Introduction

The role of multiple potential energy surfaces (PESs) and electronically nonadiabatic transitions in reaction dynamics is a topic of considerable current interest. So far, most dynamical studies have dealt with reactions of the type atom + molecule occurring on the ground state PES. In many cases, the effect of the internal (vibrational and rotational) and translational energies of the

† Present address: INFM, Sincrotrone Elettra, 34012 Trieste, Italy.

‡ Present address: Department of Molecular and Laser Physics, University of Nijmegen, 6500 GL Nijmegen, The Netherlands.



**This journal is © The Royal Society of Chemistry 1999**

reagent on the integral and differential reactive cross-sections has been examined both at the experimental and theoretical levels.[1–3] Among the various forms of energy that can be supplied to reagents, electronic energy is quite peculiar. Indeed, the extent of electronic excitation is usually such that even reactions which are strongly endoergic for the ground state species are made energetically open.[4] More importantly, the role of electronic excitation is that of driving the reaction on a PES that is different from the ground state PES and it is the different topology of the excited PESs that determines the different reactivity of the various electronic states.[4,5]

A species whose ground and excited states and their interactions are of great interest is atomic oxygen. A distinguishing feature of many atomic oxygen reactions is the interplay between the ground state PES (originating from ground state $O(^3P)$) and the first electronically excited PES (originating from the first electronically excited state $O(^1D)$, whose energy content is 190 kJ $mol^{-1}$ above the ground state), as they correlate with the same products. In fact, even though the triplet PES starts lower in energy, the singlet PES originating from the $O(^1D)$ reactant usually supports a strongly bound intermediate and therefore "crosses" the triplet surface, becoming the lower of the two up to the products.[6] Intersystem crossing (ISC) is then possible from the triplet to the singlet PES (and *vice versa*), making the dynamics that involve motion on the underlying singlet PES different from those involving motion only over the triplet PES. As a consequence, a full understanding of atomic oxygen reactions can not disregard the possibility of triplet to singlet non-adiabatic transitions.

Detailed studies on the reaction dynamics of $O(^3P)$ and $O(^1D)$have been performed pointing out their differences,[6–9] but only rarely was a direct comparison of the two possible.[10,11] Here we report on the results of a crossed beam investigation of the reaction of $CH_3I$ with both $O(^3P)$ and $O(^1D)$ under the same experimental conditions; the purpose is to assess the effect of electronic excitation on the reaction dynamics and the role and extent of ISC for this system where the presence of the heavy iodine atom is thought to facilitate its occurrence.

Thermodynamically allowed products for the reaction $O(^3P) + CH_3I$ are:

$$\rightarrow IO + CH_3 \qquad \Delta H^\circ_{298\,K} = -2.9 \text{ kJ mol}^{-1} \S \qquad (1a)$$

$$\rightarrow OH + CH_2I \qquad \Delta H^\circ_{298\,K} = -7.5 \text{ kJ mol}^{-1} \qquad (1b)$$

$$O(^3P) + CH_3I \rightarrow H + I + CH_2O \qquad \Delta H^\circ_{298\,K} = -48.1 \text{ kJ mol}^{-1} \qquad (1c)$$

$$\rightarrow I + CH_3O \qquad \Delta H^\circ_{298\,K} = -140.6 \text{ kJ mol}^{-1} \qquad (1d)$$

$$\rightarrow HI + CH_2O \qquad \Delta H^\circ_{298\,K} = -346.4 \text{ kJ mol}^{-1} \qquad (1e)$$

with the list $O(^1D) + CH_3I$ being even larger, including also the formation of $HOI + CH_2$ and $ICH_2O + H$.

Measurements of the absolute rate constants between 213 and 364 K and product yields at 298 K have been recently reported for reaction (1).[12] Channels (1a) and (1b) were found to account for 44% and 16% of the global rate constant, respectively; product yields for the minor channels are reported to be $\approx$7% for H formation, $<$3% for $CH_3O$ formation, and $<$5% for HI formation. The observation of numerous products suggested that the $O(^3P) + CH_3I$ reaction is quite complex and occurs on multiple PESs. The detailed kinetic study by Gilles *et al.*[12] has established that the $IO + CH_3$ channel in the $O(^3P)$ reaction is the dominant one and increases in importance with increasing temperature: the IO yield increases from 38% at 254 K to 58% at 370 K, while the global temperature coefficient of reaction (1) ($k_{298} = (1.8 \pm 0.2) \times 10^{-11}$ $cm^3$ $molecule^{-1}$ $s^{-1}$) shows a small negative temperature dependence providing support for formation of a long-lived collision complex. The rate constant for the reaction $O(^1D) + CH_3I$ has not been determined. However, recent kinetic studies[13] provided room temperature rate constants for the analogous reactions $O(^1D) + CH_3Cl$ and $O(^1D) + CH_3Br$, being $1.9 \times 10^{-10}$ and $1.8 \times 10^{-10}$ $cm^3$ $molecule^{-1}$ $s^{-1}$, respectively; it is reasonable to expect a similar value for $O(^1D) + CH_3I$. Argon matrix experiments[14] revealed the existence of an addition intermediate $CH_3IO$ (iodosylmethane) after the irradiation of $CH_3I \cdot O_3$ complexes; $CH_3IO$ was also seen to rearrange to either iodomethanol ($ICH_2OH$) or methyl hypoiodite ($CH_3OI$) or to eliminate HI.

§ The enthalpy of formation of IO is somewhat uncertain, with values reported in the literature ranging from $\Delta_f H^\circ_{298\,K} = 108$ kJ $mol^{-1}$ to $\Delta_f H^\circ_{298\,K} = 172$ kJ $mol^{-1}$. Here we have used $\Delta_f H^\circ_{298\,K} = 120.5$ kJ $mol^{-1}$ recently estimated by Gilles *et al.*[12] For a list of enthalpies of formation see ref. 12.

Misra *et al.*[15] used *ab initio* theory to calculate the energies and geometries of the various reaction intermediates and products involved in reactions (1), they characterized the transition states that connect the various species and have used the results to develop the singlet and triplet PES for the reactions $O(^3P,^1D) + CH_3I$. Statistical calculations[15] for the $O(^3P)$ reaction predict IO to be the dominant product below 2000 K, but other products are also possible. Fig. 1 depicts the singlet and triplet PESs for $O + CH_3I$ with ISC represented symbolically. As can be inferred from Fig. 1, $O(^3P)$ can either react on the triplet PES, giving $IO + CH_3$, or can undergo ISC to the singlet PES, forming the bound $OICH_3$ intermediate, which will decompose because of its high energy content. $O(^1D)$ will instead react on the singlet PES forming a bound $CH_3IO/CH_3OI$ intermediate that dissociates to products; ISC to the triplet PES can occur as well. The theoretical calculations suggest that ISC does not occur for the strictly collinear collisions between $O(^3P)$ and $CH_3I$ since the singlet surface is always higher in energy in linear geometry. The crossing between the triplet and singlet PESs permits access to the rich chemistry that has been observed in kinetic studies. The calculations put the barrier for isomerization of $CH_3IO$ to $CH_3OI$ above the triplet reactant asymptote, thus explaining the lack of a significant yield of $CH_3O + I$. The derived surfaces satisfactorily explain the complex kinetics and the branching ratios observed for the $O(^3P) + CH_3I$ reaction.[15]

Another reason to pursue a detailed dynamical study of the title reactions is due to their relevance in atmospheric and combustion chemistry. Indeed, the reactions of atomic oxygen, both $O(^3P)$ and $O(^1D)$, with halogenated compounds are of interest in determining the impact of the surface release of halogen-containing molecules on the atmosphere, and especially on the ozone natural balance. More specifically, while the active forms of chlorine and bromine contribute to *stratospheric ozone* depletion, it has been suggested that the *tropospheric ozone* balance may be affected significantly by iodine compounds.[16] Iodine was proposed to account also for the observed depletion of lower stratospheric ozone (below 20 km, altitudes where chlorine and bromine are not very effective for ozone destruction) at midlatitudes.[17] The main source of atmospheric iodine is natural: methyl iodide (principally), chloroiodomethane and diiodomethane are highly significant metabolic byproducts of marine biota. Although industrial sources of iodocarbons appear to be negligible compared to oceanic sources, iodocarbons generated by biomass burning could contribute to the iodine reaching the stratosphere; it is highly likely that $CH_3I$ is also released in this way because of the significant elemental abundance of iodine in plant matter. Although $CH_3I$ has a short lifetime (about 4 d) in the troposphere due to its rapid photodecomposition, and this would preclude significant transport of it into the stratosphere, research shows that convective clouds can transport insoluble material (as just iodoalkanes) very rapidly

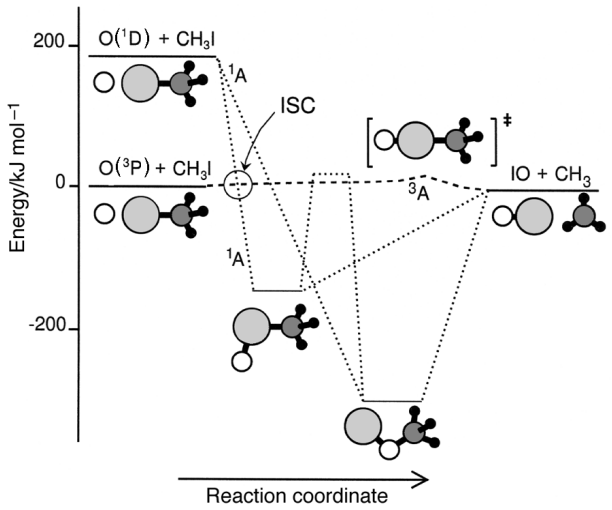


**Fig. 1** Singlet (·····) and triplet (– – –) potential energy surfaces (schematic) for the reactions $O(^3P,^1D) + CH_3I \rightarrow IO + CH_3$ with inter system crossing (ISC) indicated (the energies are taken from ref. 15).

from low altitudes to the upper troposphere and even lower stratosphere, particularly in the tropics.[17] The amount of iodine in the stratosphere is still unknown, but the work of Solomon *et al.*[17,18] demonstrates that iodine chemistry merits consideration in the studies of ozone destruction mechanisms. The main products of the reactions of $CH_3I$ with $O(^3P)$ and $O(^1D)$ are IO radicals and the possibility of rapid interhalogen reactions involving iodine (such as IO + ClO and IO + BrO)[19] could play an important role in understanding the ozone losses in the lower stratosphere at midlatitudes and in the troposphere at polar sunrise. Another important reaction in models of ozone losses in the stratosphere is $HO_2$ + IO.[20] The IO radical has been detected in the marine boundary layer very recently.[21] Finally, the reactions of $O(^3P,^1D)$ atoms with halogen containing molecules are also of relevance in the combustion chemistry of halogenated compounds, for their use as fire extinguishers (for instance, iodine containing molecules have been considered as potential substitutes for halon fire suppressants).

In previous work from this laboratory, we reported the results of direct dynamical investigations, using the crossed molecular beam (CMB) method, on the reactions of $O(^1D)$ with some halogenated molecules (HCl, HBr, HI, $CF_3Br$)[8,9,11,22–25] and of $O(^3P,^1D)$ with $H_2S$,[8–11] which are also of relevance in atmospheric and combustion chemistry. For none of them, however, was the occurrence of ISC evidenced. The group of the late Roger Grice carried out an extensive amount of work on the reactive scattering of $O(^3P)$ with halogen and interhalogen molecules,[26] and with alkyl iodides ($C_2H_5I$, $C_3H_5I$, $(CH_3)_2CHI$, $(CH_3)_3CI$)[27–29] and haloalkyl iodides ($CF_3I$, $CF_3CH_2I$, $CH_2ICl$)[30–32] giving some evidence of ISC to the singlet PES.[27–33] In this contribution we report the first dynamical study of the reaction of oxygen atoms with the prototype alkyl iodide, $CH_3I$, which makes it possible to compare directly the dynamic behavior of $O(^3P)$ and $O(^1D)$ and to determine the extent of triplet to singlet ISC. Our findings are discussed in the light of recent *ab initio* calculations[15] of the triplet and singlet PESs. Calculations based on phase space theory are performed and compared with experimental results.

## II. Experimental

The scattering experiments were carried out in a universal crossed molecular beam apparatus described in detail elsewhere.[8,11,34] Fig. 2 shows a schematic diagram of the set-up. Briefly, two supersonic beams of the reactants, doubly differentially pumped and well collimated in angle and velocity, are crossed at 90° under single collision conditions in a large scattering chamber kept

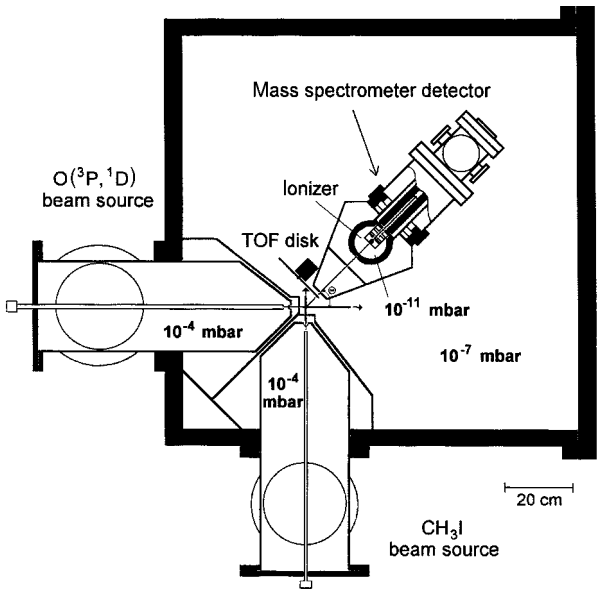


**Fig. 2** Cross-sectional view (from the top) of the crossed molecular beam instrument with rotating mass spectrometer detector and time-of-flight analysis.

below $5 \times 10^{-7}$ mbar. The angular and velocity distributions of the reaction products are recorded by a rotatable, triply differentially pumped, ultrahigh vacuum ($10^{-11}$ mbar) electron impact ionization quadrupole mass spectrometer detector using time-of-flight (TOF) analysis. We have exploited the capability of generating intense and continuous supersonic beams of oxygen atoms, containing mostly $O(^3P)$ with a small percentage of $O(^1D)$, by radio-frequency (rf) discharge[8,11,35,36] in a water-cooled quartz nozzle (0.24 mm diameter) at high pressure (220 mbar) of dilute (4%) $O_2$ (isotopically enriched in $^{18}O_2$) in He gas mixture and high rf power (300 W). The oxygen beam has a peak velocity of 2625 m $s^{-1}$, an angular divergence of 2.3° and a speed ratio of 6.7, as measured from single-shot TOF analysis. Experiments were carried out at two different collision energy ($E_c$) values, 55.2 and 64.0 kJ $mol^{-1}$, which were obtained by using beams of $CH_3I$ having different velocities. For the lower $E_c$, a 25% mixture of $CH_3I$ seeded in Ar at 0.6 bar was expanded through a 0.1 mm stainless-steel nozzle, kept at 470 K to minimize cluster formation; the peak velocity and speed ratio were 564 m $s^{-1}$ and 11. For the high $E_c$, a 7% mixture of $CH_3I$ in He at 2.5 bar was used; the nozzle temperature was 570 K, the peak velocity 1314 m $s^{-1}$ and the speed ratio 13. The $CH_3I$ beam angular divergence was 2.1°.

The use of a beam of $^{18}O$ was mandatory for the success of these experiments, in which the main reaction product is IO. In fact, the natural abundance of $^{13}C$ in the $CH_3I$ beam would produce a strong interference at the mass of the IO product ($m/z = 143$) making its detection difficult due to the elastically scattered $^{13}CH_3I$. Use of $^{18}O$ allowed us to detect the $^{18}OI$ product at $m/z = 145$, which can be well separated in mass from the $m/z = 143$ elastic contamination.

Under our experimental conditions we have observed only the IO product from the title reactions, which is indeed the major reaction product.[12] HOI formation was not seen to occur. Product detection for the other possible reaction channels is kinematically unfavored or hindered by dissociative ionization of elastically scattered $CH_3I$ in the ionizer. Angular distributions of the IO product were obtained by taking at least five scans of 30–60 s counts at each angle (every 4°), depending on signal intensity. The oxygen beam was modulated at 160 Hz with a tuning fork chopper for background subtraction. The signal-to-noise ratio was about 70 and 90 for the low and high $E_c$ experiments, respectively. The velocity distributions of the products were obtained at selected laboratory angles using the cross-correlation TOF technique[37] with four 127 bit pseudo-random sequences. High time resolution was achieved by spinning the TOF disk, located at the entrance of the detector, at 246.1 Hz, which corresponds to a dwell time of 8 μs $channel^{-1}$. The flight length was 24.6 cm. Counting times varied from 15 to 60 min depending upon the signal intensity.

The scattering measurements were carried out in a laboratory (lab) system of coordinates, while for the physical interpretation of the scattering process it was necessary to transform the data (angular, $N(\Theta)$, and velocity, $N(\Theta, v)$, distributions) to a coordinate system moving with the center of mass (c.m.) of the colliding system.[38] The transformation is fairly straightforward and the relation between lab and c.m. fluxes is given by $I_{lab}(\Theta, v) = I_{c.m.}(\theta, u)v^2/u^2$ (where $\Theta$ and $v$ are the lab angle and velocity, respectively, and $\theta$ and $u$ are the corresponding c.m. quantities), *i.e.*, the scattering intensity observed in the laboratory is distorted by the transformation Jacobian $v^2/u^2$ from that in the c.m. system.[38] Since the electron impact ionization mass spectrometric detector measures the number density of the products, $N(\Theta)$, not their flux, the actual relation between the lab density and the c.m. flux is given by $N_{lab}(\Theta, v) = I_{c.m.}(\theta, u)v/u^2$.

Because of the finite resolution of the experimental conditions, *i.e.*, the finite angular and velocity spread of the reactant beams and angular resolution of the detector, the lab to c.m. transformation is not single valued and, therefore, analysis of the laboratory data is carried out by forward convolution procedures over the experimental conditions of trial c.m. distributions (*i.e.*, c.m. angular and velocity distributions are assumed, averaged and transformed to the lab frame for comparison with the data). The final outcome is the generation of velocity flux contour maps of the reaction products, *i.e.*, a plot of intensity as a function of the angle and velocity in the c.m. system, $I_{c.m.}(\theta, u)$. These contour maps can be regarded as *images* of the reaction.

## III. Results and analysis

Laboratory angle distributions of IO product number density at $E_c = 55.2$ kJ $mol^{-1}$ and $E_c = 64.0$ kJ $mol^{-1}$ are shown in Figs. 3 and 4 together with the corresponding velocity vector

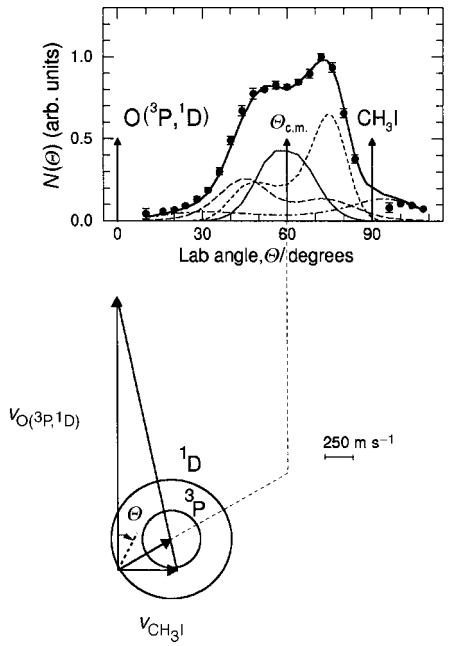


**Fig. 3** Laboratory angular distribution (●) of the IO product at $E_c = 55.2$ kJ mol$^{-1}$ from the reactions $O(^3P,^1D) + CH_3I \rightarrow IO + CH_3$. The circles in the velocity vector ("Newton") diagram delimit the maximum velocity that the IO product can attain on the basis of energy conservation if all the available energy for the triplet and the singlet reactions goes into product translational energy. The separate contributions to the total lab angle distribution (———) from the triplet direct reaction (-------), the triplet reaction *via* ISC (——), the singlet-direct reaction (–·–·–·), and the singlet reaction *via* osculating complex ( — — ) are shown.

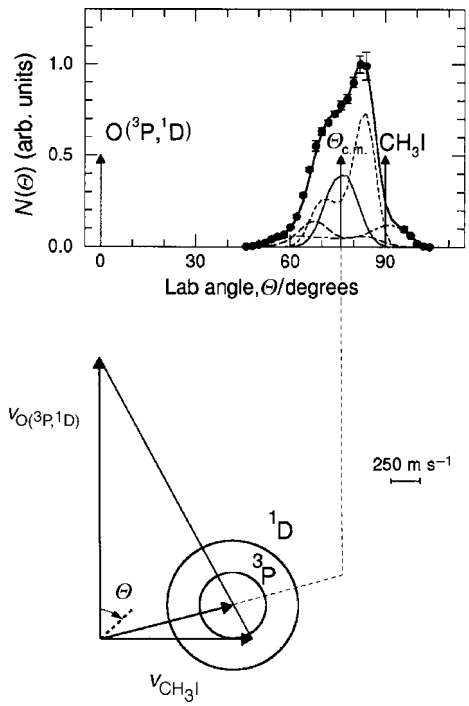


**Fig. 4** As for Fig. 3, but at $E_c = 64.0$ kJ mol$^{-1}$.

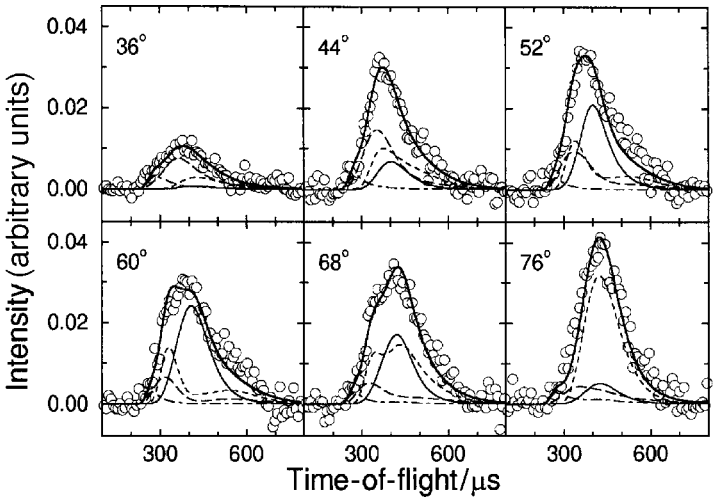


**Fig. 5** Time-of-flight distributions of the IO product from the reactions $O(^3P,^1D) + CH_3I \rightarrow IO + CH_3$ at the indicated lab angles at $E_c = 55.2$ kJ mol$^{-1}$. Best fit global and partial distributions (lines as in Fig. 3) from the various triplet and singlet micromechanisms are shown.

("Newton") diagrams. The error bars indicated represent $\pm 1$ standard deviation. The corresponding TOF spectra at selected lab angles are shown in the Figs. 5 and 6; they have been normalized to the relative intensities at each angle. Because of the increased $CH_3I$ beam velocity, the c.m. position moves from about $\Theta_{c.m.} = 60°$ at the low $E_c$ to about $\Theta_{c.m.} = 76°$ at high $E_c$ (see Figs. 3 and 4). As the Newton diagrams show, the laboratory angle ranges within which the IO product formed from the $O(^3P)$ reaction can be scattered are limited (on the basis of linear momentum constraints and energy conservation) to angles from $\Theta \approx 33°$ to 88° at $E_c = 55.2$ kJ mol$^{-1}$ and from $\Theta \approx 62°$ to 90° at $E_c = 64.0$ kJ mol$^{-1}$. In contrast, owing to the extra 190 kJ mol$^{-1}$ of energy, the IO product formed from the $O(^1D)$ reaction can spread over a much broader laboratory angle range. The measured lab angle distributions at both $E_c$ values show that the product is distributed on both sides of $\Theta_{c.m.}$ and have both a peak and a shoulder at angles close to $\Theta_{c.m.}$.

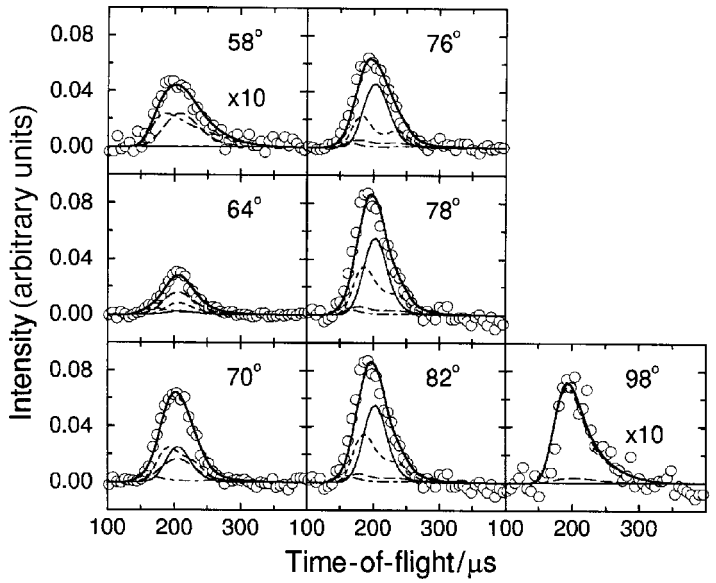


**Fig. 6** As for Fig. 5, but at $E_c = 64.0$ kJ mol$^{-1}$.

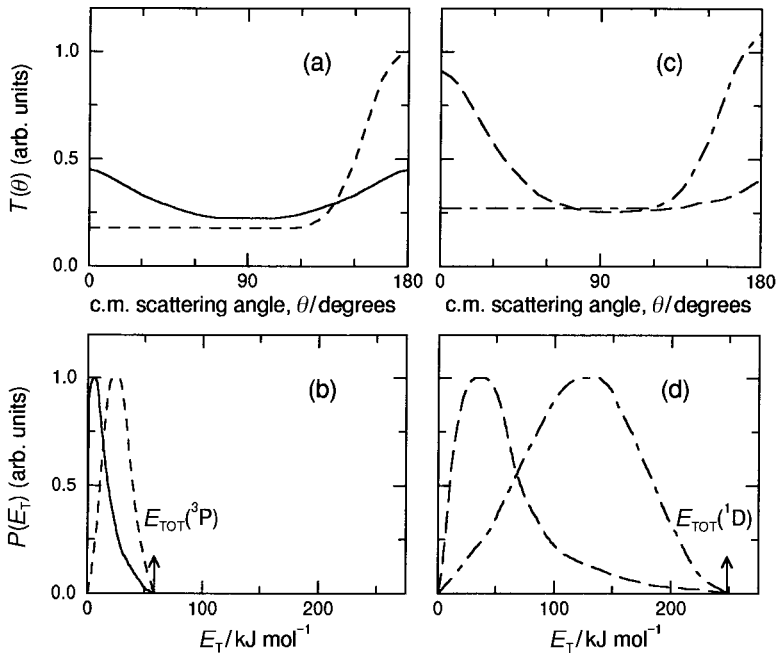


**Fig. 7** Best fit center of mass product angular (top) and translational energy (bottom) distributions for the $O(^3P)$ reaction [(a), (b)] and for the $O(^1D)$ reaction [(c), (d)] at $E_c = 55.2$ kJ mol$^{-1}$.

Two remarkable features are the peak sharpness and the large width of the two angular distributions; in particular, the tails of the angular distributions extend well beyond the range of the $O(^3P)$ reaction, and they cannot be reproduced during data analysis unless a significant contribution from the $O(^1D)$ reaction is invoked. Analogously, the TOF data reveal contributions from both the $O(^3P)$ and the $O(^1D)$ reactions. For instance, the fast part of the $\Theta = 36°$ TOF spectrum at $E_c = 55.2$ kJ mol$^{-1}$ can energetically only come from the $O(^1D)$ reaction, while the whole spectrum at $\Theta = 98°$ for $E_c = 64.0$ kJ mol$^{-1}$ can only originate from the $O(^1D)$ reaction. Preliminary attempts at fits, which invoked a set of uncoupled angular and translational energy distributions for each electronic state of oxygen, proved unsuccessful since the range of velocities that the products reached turned out not to be the same in different directions for both reactions. To be specific, the lab distributions measured suggest by themselves that two competing micromechanisms are involved for both the $O(^3P)$ and the $O(^1D)$ reactions, and this led us to use four distinct contributions (two for the $O(^1D)$ and two for the $O(^3P)$ reaction) in the forward convolution trial and error fitting procedure to express the global c.m. product flux, according to:

$$I_{c.m.}(\theta, E_T) = [T(\theta)P(E_T)]_{triplet\text{-}direct} + \alpha[T(\theta)P(E_T)]_{triplet\text{-}complex} + \beta[T(\theta)P(E_T)]_{singlet\text{-}complex} + \gamma[T(\theta)P(E_T)]_{singlet\text{-}direct}$$

where $T(\theta)$ and $P(E_T)$ are the c.m. angular and translational energy distributions (assumed to be uncoupled), and complex and direct refer to micromechanisms by long lived (or osculating) complex formation and by direct reaction, respectively. The coefficients $\alpha$, $\beta$, and $\gamma$ weigh the various contributions with respect to the first one and were treated as adjustable parameters during the fitting procedure. The best fit values are $\alpha \approx 0.5$ and $\beta \approx \gamma \approx 1$ at $E_c = 55.2$ kJ mol$^{-1}$; the values obtained at $E_c = 64.0$ kJ mol$^{-1}$ are very similar with only $\alpha$ being a little smaller ($\approx$0.4). They correspond to the following ratios amongst the integral reaction cross-sections: $\sigma_{triplet\text{-}direct}/\sigma_{triplet\text{-}complex} = 0.9$ and 1.1 for the low and high energy experiment, respectively, and $\sigma_{singlet\text{-}direct}/\sigma_{singlet\text{-}complex} \approx 1$ at both $E_c$. The reaction cross-section for each micromechanism is

obtained by integrating over the corresponding differential cross-section $\sigma = 2\pi \int_0^{\pi} T(\theta)\sin\theta \, d\theta$ and accounting for the corresponding weight factor. The resulting weight of the $O(^1D)$ contribution to the total c.m. function is slightly larger than that from $O(^3P)$. This is not surprising, since the oxygen beam largely consists of $O(^3P)$, but the rate constant for $O(^1D)$ should be larger than that for $O(^3P)$.

Fig. 7 depicts the set of best fit c.m. product angular and translational energy distributions for the two micromechanisms for the $O(^3P)$ and $O(^1D)$ reactions at $E_c = 55.2$ kJ mol$^{-1}$. The best fit c.m. functions at $E_c = 64.0$ kJ mol$^{-1}$ are very similar to those at the lower $E_c$, *i.e.*, the $P(E_T)$ values scale with the slight difference in total available energy, the only noticeable difference being that the forward $O(^1D)$ component is slightly more forward than at lower $E_c$. Fig. 8 reports the product velocity flux contour maps at $E_c = 55.2$ kJ mol$^{-1}$ for the four separate contributions. The c.m. contour maps $I_{c.m.}(\theta, u)$ have been obtained after a straightforward transformation to convert the flux distribution in the energy space $I_{c.m.}(\theta, E_T)$ into that in the velocity space $I_{c.m.}(\theta, u)$. The heavy solid line in Figs. 3–6 represents the total angular distributions calculated from the best fit c.m. functions, while the light solid, long dashed, dashed and dashed dotted lines correspond to the four separate contributions.

As depicted by Fig. 7(a) and (b) and in the c.m. flux contour maps of Fig. 8 (bottom left), one of the two $O(^3P)$ micromechanisms is characterized by a symmetric, backward/forward peaked, angular distribution that is quite polarized (*i.e.*, the intensity in the forward and backward directions is much larger than in the sideways direction), and by a product translational energy distribution peaking at low energy. These findings are attributed to the reaction proceeding through the formation of a long-lived $CH_3IO$ complex following ISC from the triplet to the singlet PES. The singlet adduct formed after ISC has an internal energy of about 220 kJ mol$^{-1}$ (the well depth with respect to $IO + CH_3$ products, $\approx$160 kJ mol$^{-1}$, plus the exoergicity and the relative collision energy) and will dissociate to products. The symmetric c.m. angular distribution suggests that the lifetime of the complex is larger than its rotational period. This is confirmed by estimating the ratio of the lifetime $\tau$ to the rotational period $\tau_r$ for the singlet $CH_3IO$ complex from the RRKM

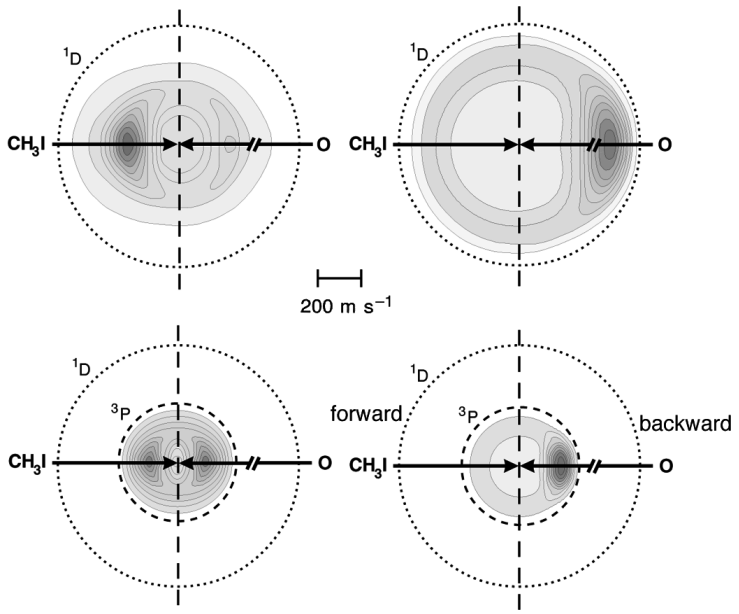


**Fig. 8** Center of mass polar flux (velocity and angle) contour maps of the IO product at $E_c = 55.2$ kJ mol$^{-1}$ showing the IO distribution from the $O(^1D)$ reaction *via* an *osculating complex* (top left), from the $O(^3P)$ reaction *via* ISC to the singlet PES and *long-lived complex* formation (bottom left), and from the $O(^1D)$ and $O(^3P)$ reactions occurring with direct (*rebound*) mechanism (top and bottom right, respectively).

formula[33,39,40]

$$\tau \approx \nu^{-1}\{(E_c - \Delta_r H^\circ + E_0)/(E_c - \Delta_r H^\circ)\}^{s-1} \quad (2)$$

and from the relation

$$\tau_r = 2\pi I/L_{max} \quad (3)$$

where $E_0$ is the well depth ($\approx$160 kJ mol$^{-1}$) of the complex, $\Delta_r H^\circ$ is the reaction enthalpy at 0 K, $I$ is the moment of inertia of the complex, and $L_{max}$ is the maximum initial orbital angular momentum ($L_{max} = \mu v_r b_{max}$, where $\mu$ is the reduced mass of the reactants, $v_r$ is the initial relative velocity, and $b_{max}$ is the maximum impact parameter). For $E_c = 55.2$ kJ mol$^{-1}$, when using $L_{max}$ of $\approx 152h/(2\pi)$ (corresponding to a maximum impact parameter $b_{max} = 2.3$ Å), a moment of inertia $I \approx 2.13 \times 10^{-45}$ kg m$^2$, a geometric mean vibrational frequency $\nu = 4.0 \times 10^{13}$ s$^{-1}$, and an effective number of modes $s = 6$ corresponding to the heavy atom motion with frequencies estimated from the *ab initio* calculations[15] for $CH_3IO$ and the spectroscopic values for $CH_3I$, the calculated $\tau$ is 19 ps and $\tau_r$ 0.8 ps. Therefore, $\tau/\tau_r$ is $\approx$23, which indicates that the complex lives a sufficiently long time to lose the memory of the initial approach direction of the reactants.

As can be clearly seen in Figs. 7(a) and (b) and 8 (bottom right), the second micromechanism from O($^3$P) is characterized by a preferentially backward peaked c.m. angular distribution with a high product recoil energy and it is attributed to a direct abstraction reaction over the triplet PES (see Fig. 1 and next section).

The average product translational energy, defined as $\langle E_T \rangle = \Sigma P(E_T)E_T/\Sigma P(E_T)$, is 14 kJ mol$^{-1}$ for the first mechanism and 26 kJ mol$^{-1}$ for the second one, *i.e.*, the percentage of the total available energy, $E_{TOT}$, released as product translational energy, is very different in the two cases. In this type of experiment, the total available energy is given by $E_{TOT} = E_c - \Delta_r H^\circ + E_{int}$, where $\Delta_r H^\circ$ is the enthalpy of reaction and $E_{int}$ is the internal energy of the reactants, namely, the internal energy of $CH_3I$. Because of the significant relaxation occurring during supersonic expansion, the rotational energy of $CH_3I$ does not contribute significantly to the total available energy (the low frequency vibrational modes may be excited at the nozzle temperature and may not be completely relaxed in the beam, but their energy weighs little and therefore can be neglected). As we have already seen, the enthalpy of reaction is not accurately known, since the enthalpy of formation of the IO radical has not been accurately established yet (see ref. 41 for a recent review on the enthalpies of formation and other properties of iodine oxides). We have used the values recently derived from a crossed beam study[25] of the reaction O($^1$D) + HI $\rightarrow$ IO + H, namely $\Delta_r H^\circ$ (0 K) = 121.3 kJ mol$^{-1}$, which is in agreement with the values derived by Radlein and coworkers,[42] and Buss and coworkers,[43] with a recent theoretical estimation[44] and with the $T = 298$ K value reported by Gilles and coworkers[12] and by others.[45] With this value of $\Delta_r H^\circ$ the resulting average fractions of energy in translation are 24% and 44% of the total available energy for the complex forming mechanism and the direct abstraction mechanism, respectively.

The O($^1$D) reaction was also found to occur *via* two micromechanisms: the first one is witnessed by the forward peaked c.m. angular distribution with a moderate fraction of recoil energy (about 24% at both $E_c$ values), while the second one exhibits a backward peaked c.m. angular distribution (reflecting a *rebound* reaction) with a large fraction (about 50% at both $E_c$ values) of product recoil energy (see Fig. 7(c) and (d) and Fig. 8(top)). The forward peaked angular distribution may well reflect the formation of an *osculating complex* following O($^1$D) addition and/or insertion along the singlet PES. In fact, according to the osculating complex model for chemical reaction,[46] a forward intensity enhancement is expected when the complex lifetime is a fraction of, or comparable to, its rotational period. An estimate of the ratio between the lifetime of the decomposing complex and its rotational period, $\tau/\tau_r$, can be obtained from the observed $T(\theta)$ asymmetry by means of $T(180^\circ)/T(0^\circ) = \exp(-\tau_r/2\tau)$, where $T(0^\circ)$ and $T(180^\circ)$ are the values assumed by the $T(\theta)$ function at the two poles. From the experimental asymmetry $T(180^\circ)/T(0^\circ) = 0.32$ a ratio for $\tau/\tau_r = 0.44$ is derived. This value can be compared with the $\tau/\tau_r$ value of 0.5 (for $CH_3IO$) and 1.6 (for $CH_3OI$) obtained from eqns. (2) and (3) when using an initial orbital angular momentum $L_{max} \approx 200h/(2\pi)$ and the proper moment of inertia ($I_{max} = 2.77 \times 10^{-45}$ kg m$^2$ for $CH_3OI$). The $L_{max}$ value corresponds to $b_{max} \approx 3$ Å, obtained assuming the O($^1$D) reaction without any entrance potential barrier and dominated by dispersion forces.[1]

The backward peaked angular distribution from the $O(^1D)$ reaction reflects a direct reaction mechanism in which the $O(^1D)$ atom approach to the $CH_3I$ molecule on the iodine side is nearly collinear at relatively small impact parameters, thereby not experiencing the deep potential well and giving rise to a rebound dynamics. The large fraction (50%) of available energy released as recoil energy witnesses the strong repulsion among the separating moieties in the exit channel. Similar results were observed for the $O(^1D) + HX \rightarrow XO + H$ (X = Cl, Br) reactions, where the backward scattered XO was attributed to direct abstraction of the halogen atom, with rebound dynamics *via* H–X–O configurations.[22,23]

Regarding the accuracy of the best fit c.m. distributions, the fit of the laboratory data has proved to be quite sensitive to the rise and the peak position of the $P(E_T)$ values, while slightly less sensitive to the fall-offs. The backward/forward ratios of the asymmetric angular distributions are within $\pm 10\%$.

**Phase space theory (PST) calculations**

It is well established that phase space calculations[47] offer a method of predicting the product angular and translational energy distributions arising from a long-lived collision complex dissociating without an exit barrier and, by comparison with experiment, of assessing the extent of energy randomization.

For the reaction between $O(^1D)$ and $CH_3I$, and, in relation to the complex forming mechanism, we have assumed the following.

(1) The reagent $CH_3I$ is in its rovibrational ground state.

(2) The probability of the formation of fragments other than $IO + CH_3$ is negligible.

(3) The interaction forces between the fragments (either the reagents or the products) are of the dispersion type. The corresponding potential energy $V(R)$ is given by $V(R) = -C_6/R^6$ where $R$ is the distance between fragments and $C_6$ is the dispersion coefficient (see ref. 48).

(4) The lifetime of the intermediate complex is sufficiently long for a complete energy randomization to be achieved. Such an assumption, together with assumption (3), makes equally likely all of the final states available to the system,[48] subject to conservation of the total energy and the total angular momentum.

(5) The internal vibrations of the fragments are treated quantum mechanically whereas the rotational and translational motions are treated by classical mechanics.[49] Because of assumption (4), all internal vibrations of the final fragments are taken into account.

In the case of the reaction between $O(^3P)$ and $CH_3I$ proceeding through ISC, the dynamics in the entrance channel are not governed by long range forces. Instead, we have assumed the following.

(6) Complex formation takes place *via* intersystem crossing. As shown by Misra *et al.*,[15] ISC is most probable in the entrance channel at an O–I distance of $\approx 2.3$ Å and a bent O–I–C configuration of 109°, for which the potential energy $E_0$ is equal to $\approx 30$ kJ mol$^{-1}$. Using the angular dependent line of center (ADLOC) model,[50] a reasonable estimation of the opacity function can then be made, from which a distribution of the orbital angular momentum consistent with complex formation is deduced.

The remaining assumptions are the same as previously. The technical details of the calculations will be given elsewhere.[51]

The product translational energy and angular distributions for the $O(^3P)$ reaction calculated from PST show very good agreement with the experimental distributions (see Fig. 9 for $E_c = 55.2$ kJ mol$^{-1}$). The symmetrical angular distribution corresponds to a lifetime of the collision complex of many rotational periods and the statistical product translational energy distribution indicates that there is a complete energy randomization in the complex before it decomposes to products. This confirms that an IO component characterized by a symmetric angular distribution arises from a long-lived singlet $CH_3IO$ complex formed by ISC from the triplet to the singlet PES in small impact parameter collisions with $b < 2.3$ Å. Similar good agreement between extended PST calculations and experimental product angular and translational energy distributions was also reported in a study of the $O(^3P) + C_2H_5I \rightarrow IO + C_2H_5$ reaction at $E_c = 16$ kJ mol$^{-1}$, which was found to proceed by ISC at that energy.[27] It is interesting to note that for the same reaction at higher $E_c$ of 51 kJ mol$^{-1}$, a ratio of about one between the direct dynamics over the triplet PES

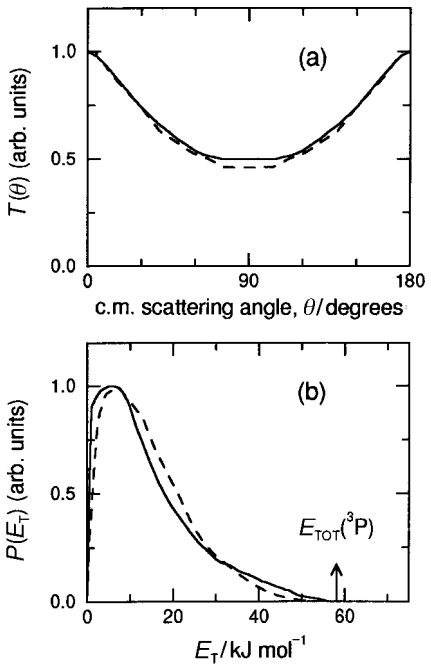


**Fig. 9** Product angular distribution and translational energy distribution for IO scattering at $E_c = 55.2$ kJ $mol^{-1}$ calculated from phase space theory (dashed curve) compared with the experimental distributions (solid line).

and ISC to the singlet PES was determined, which is very similar to that found for $O(^3P) + CH_3I$ in the present study. For the reaction $O(^3P) + CH_2ICl \rightarrow IO + CH_2Cl$ at $E_c = 46$ kJ $mol^{-1}$, the ratio $\sigma_{ISC}/\sigma_{direct}$ is $\approx 0.35$ and, notably, the product angular and translational energy distributions[32] bear a close resemblance to those derived here for $O(^3P) + CH_3I$.

The PST calculations for the $O(^1D)$ reaction, assumed to proceed *via* a long-lived complex, give a product translational energy distribution corresponding to about 17% of recoil energy when all seven vibrations are assumed to participate in the intramolecular energy redistribution. This number is somewhat lower than the experimental value of 24% and suggests that collision complexes that persist for only one rotational period do not achieve complete energy equilibration.

## IV. Discussion

The c.m. product angular and translational energy distributions shown in Fig. 7 allow an evaluation of the dynamical influence of the PESs and of the kinematic constraints on the reactions $O(^3P,^1D) + CH_3I \rightarrow IO + CH_3$. The *ab initio* calculations of Misra *et al.*[15] and Fig. 1 form the basis of the following discussion.

### $O(^3P)$ reaction dynamics

Regarding the backward/forward symmetry of the IO angular distribution from the $O(^3P)$ reaction, this is the expected result for reactions proceeding through the formation of a long-lived complex, which implies the existence of a deep potential well supporting a bound intermediate. As shown by recent *ab initio* calculations[15] the triplet surface is not characterized by the presence of such a bound intermediate; however, if a considerable amount of the reactive encounters of $O(^3P)$ do not proceed adiabatically on the triplet PES, but undergo a nonadiabatic transition from the

triplet to the singlet PES, the deep well of the bound $CH_3IO$ singlet intermediate may be accessed. These suggestions are in line with what was proposed by Grice and coworkers in their studies on a series of $O(^3P)$ + alkyl iodide[27–29] and also haloalkyl iodide[30–32] reactions. These authors found that direct dynamics over the triplet PES is responsible for back scattered IO product formed with high translational energy as result of small impact parameter collisions, whereas ISC to the singlet PES, supporting a long-lived intermediate, yields backward/forward scattered IO product with low translational energy. For alkyl iodide reactions, crossed molecular beam (CMB)[27] and Fourier transform infrared emission studies[52] proved the formation of singlet HOI product, indicating that HOI is formed *via* a triplet to singlet ISC, followed by passage through a singlet intermediate and a five-member ring transition state for the intramolecular abstraction of a $\beta$-hydrogen. Recent *ab initio* calculations on $O(^3P,^1D) + C_2H_5I$ support this picture.[53] In contrast, for the simplest alkyl iodide, $CH_3I$, investigated here, the spin-forbidden channel leading to HOI formation cannot occur because of the lack of a $\beta$-hydrogen in $CH_3I$.

The ratio of cross-sections between the triplet reaction *via* ISC and the direct triplet reaction is $\sigma_{ISC}/\sigma_{dir} \approx 1.1$ at $E_c = 55.2$ kJ mol$^{-1}$ and $\approx 0.9$ at $E_c = 64.0$ kJ mol$^{-1}$. That is, the direct abstraction reaction increases with increasing collision energy. An increase of the direct mechanism contribution to the total reaction could be explained with the presence of a small barrier along the triplet PES. Even though such a barrier was not identified by *ab initio* calculations,[15] we recall that a similar trend was also observed in studies of the series $O\,^3P + RI$ ($R = C_2H_5$, $(CH_3)_2CH$, and $(CH_3)_3C$).[27–29] For the system most closely related to the present study, namely the $O(^3P) + C_2H_5I$ reaction, the IO angular distribution was found[27] to be symmetric at low $E_c$, while it started to show some preferred backward scattering at $E_c = 36$ kJ mol$^{-1}$, suggesting that a new channel opens up at this energy since the system has enough energy to surmount the barrier to IO formation on the triplet PES. Theoretically,[53] the barrier on the triplet PES is found to be much larger than the experimental value. On the contrary, since the triplet/singlet crossing is located below the energy of the reactants, the ISC channel is open at any $E_c$. Stevens *et al.*[53] have quantified the spin–orbit coupling between the singlet and the triplet states at the crossing for the $O(^3P) + C_2H_5I$ system. The calculated value is 2.5 kJ mol$^{-1}$, a substantial value; a similar result can be expected for $O(^3P) + CH_3I$ as well.

In our experiment the total available energy for the $IO + CH_3$ products is 58.2 kJ mol$^{-1}$ at the lowest $E_c$. Since for the micromechanism *via* ISC, 25% of this energy goes as product recoil energy, the remaining 75% is channeled into internal excitation of the molecular fragments. The internal energy of the products can be rovibrational energy for both IO and $CH_3$; in addition, IO can be formed in both $^2\Pi_{3/2,\,1/2}$ spin–orbit states (spin–orbit splitting of IO ($^2\Pi_{3/2,\,1/2}$) is 25.1 kJ mol$^{-1}$ and the vibrational spacing about 8.4 kJ mol$^{-1}$).[41] Rotational excitation of the fragments should be relatively low, since the moment of inertia of $CH_3$ is small. Hence, there should be a considerable amount of vibrational excitation; in particular, the $\nu_2$ umbrella mode of $CH_3$ is expected to be considerably excited because of the change in geometry from tetrahedral to trigonal planar in proceeding from reactants to products. IO will likely be formed mainly in the ground electronic state $^2\Pi_{3/2}$ and only the lowest vibrational levels will be populated. Correlation diagrams for spin multiplet states of $O(^3P_{2,1,0})$ atoms reacting with alkyl iodide molecules in the collinear and in the bent configuration (with Renner–Teller interaction) (see Fig. 11 of ref. 27 and Fig. 9 of ref. 28) indicate that the most favorable channel should be that leading to $IO(^2\Pi_{3/2}) + CH_3(^2A_2'')$. However, nonadiabatic coupling may readily take place in the exit channel in this multisurface system containing the heavy iodine atom, as already observed in the reaction $O(^1D) + HCl \rightarrow ClO(^2\Pi_{3/2,\,1/2}) + H$.[54]

The significant polarization of the symmetric c.m. angular distribution ($T(\theta = 90°)/T(\theta = 0°) = 0.5$) for the $O(^3P)$ reaction proceeding *via* ISC and long-lived complex formation indicates a significant correlation between the initial and final orbital angular momenta $\boldsymbol{L}$ and $\boldsymbol{L}'$ (*i.e.*, $\boldsymbol{L}$ and $\boldsymbol{L}'$ are parallel or antiparallel). It is worth mentioning that the disposal of angular momentum is intimately connected with the molecular mechanism of the reaction, as was pointed out long ago by Herschbach.[55] Because the $CH_3I$ reactant is produced in a supersonic expansion, the rotational angular momentum $\boldsymbol{j}$ is quite small and the orbital angular momentum $\boldsymbol{L}$ becomes the total angular momentum $\boldsymbol{J}$. Prior to separation of the complex to products, the rotational angular momentum of the complex equals $\boldsymbol{J}$ and the almost prolate nature of the complex require that $k$, the projection of $\boldsymbol{J}$ on the symmetry axis, must be small. Under these circumstances, the

complex rotates in a plane perpendicular to $\boldsymbol{J}$ and the products are expected to be emitted isotropically in this plane. Since the mass of the departing $CH_3$ is very similar to that of the O atom which attaches to the heavy I atom, one would expect a large fraction of the total angular momentum to be disposed primarily as product orbital angular momentum $\boldsymbol{L}'$. This fact, coupled with the fact that $\boldsymbol{L}$ is perpendicular to $\boldsymbol{v}$ (the relative velocity vector) creates the 1/sin $\theta$ form factor consistent with forward/backward peaking of the c.m. angular distribution.

The backward peaked angular distribution of the direct $O(^3P)$ reaction mechanism indicates that the preferred geometry for reaction on the triplet PES is nearly collinear O–I–$CH_3$. The *ab initio* calculations[15] find that for collinear geometry the triplet PES always lies below the singlet PES, and therefore ISC cannot occur. The same calculations predict a triplet/singlet crossing as the system deviates from collinearity, which allows ISC to occur more readily for bent triplet geometry. The large fraction (44%) of available energy appearing as product recoil energy indicates a strong repulsion between the products in the exit valley of the PES.

### $O(^1D)$ reaction dynamics

The forward peaked IO angular distribution describing one of the two competitive micromechanisms of the $O(^1D)$ reaction (see Fig. 7(c) and the c.m. velocity IO contour maps depicted in Fig. 8 (top left)) suggest that part of the $O(^1D)$ reaction proceeds through an osculating complex, *i.e.*, formation of a singlet complex that lives only a fraction of, or a time comparable to, its rotational period, following $O(^1D)$ addition to iodine or insertion into the C–I bond along the singlet PES. In fact, because of the large exoergicity of the $O(^1D)$ reaction, the total energy available to the reactants is much larger than the binding energy of the complex, and consequently the complex lifetime reduces strongly (see eqn. (2)), thus giving rise to an osculating complex. From the RRKM formula, one obtains lifetime values of 0.3 and 1.3 ps for the $CH_3IO$ and $CH_3OI$ complexes, respectively, from the $O(^1D)$ reaction, which are significantly shorter than the value of 19 ps obtained for the $CH_3IO$ complex from the $O(^3P)$ reaction *via* ISC. The $\tau/\tau_r$ ratio at $E_c =$ 55.2 kJ mol$^{-1}$ obtained using eqns, (2) and (3) is $\approx$0.5 for the singlet $CH_3IO$ complex and $\approx$1.6 for $CH_3OI$. A comparison with the experimental ratio of 0.44 might suggest that the $CH_3IO$ isomer is that mainly involved (following $O(^1D)$ addition to $CH_3I$); however, because of the numerous approximations of the model we cannot rule out that the $CH_3OI$ isomer also plays a role (following $O(^1D)$ insertion into the I–$CH_3$ bond and/or interconversion of $CH_3IO$). The fraction (24%) of energy released as product recoil energy is similar to that of the $O(^3P)$ reaction *via* ISC, but is somewhat larger than the value of 17% predicted by phase space calculations assuming a long-lived complex and energy randomization. We therefore can envisage that energy randomization is not complete within the time of about one rotational period. For the $O(^1D)$ reaction large electronic and vibrational excitation of the products is possible, because of the much larger energy available. Extensive nonadiabatic effects in the exit channel are also likely, which can lead to a non-statistical population of spin–orbit states of $IO(^2\Pi)$.

It is interesting to compare the c.m. product angular distribution of the reaction $O(^1D) + CH_3I \rightarrow IO + CH_3$ proceeding *via* an osculating complex with that of the reaction $O(^1D) + HI \rightarrow IO + H$ studied previously,[25] which proceeds *via* an osculating complex as well. The former is considerably forward peaked, but it is also suggestive of a significant polarization (as confirmed by PST calculations), while the latter is almost isotropic, although with preferred forward scattering. In these two reactions a notable difference in the disposal of the rotational energy of the complex was observed.

For comparable $E_c$, about 46% of product recoil energy is seen for $O(^1D) + HI \rightarrow IO + H$ (a) and only 24% for $O(^1D) + CH_3I \rightarrow IO + CH_3$ (b) (the exothermicities are equal to 126 and 188 kJ mol$^{-1}$ for reactions (a) and (b), respectively). Such a fact can be explained as follows. First of all, the distribution of the reagent orbital angular momentum $\boldsymbol{L}$ consistent with the formation of the complex is roughly the same for both processes since the mechanical parameters responsible for this distribution have close values. Second, the maximum value $L'_m$ (consistent with the available energy $E'$) is much lower in case (a) than in case (b), mainly due to the fact that the reduced mass of H with respect to IO is about 15 times less than that of $CH_3$ with respect to IO. Therefore, the average value $\langle L/L'_m \rangle$ is larger in case (a) than in case (b). Since values of $L'$ close to $L'_m$ lead to large recoil energies, the recoil energy distribution is expected to be more excited in case (a) than

in case (b). If, in addition to that, we take into account the rovibrational degrees of freedom of $CH_3$ which can consume part of the available energy, we understand that all factors favor more translational excitation between IO and H than between IO and $CH_3$.

It is worth noting that PST calculations[56] find a fraction of the energy in translation form for $O(^1D) + HI$, in agreement with experiment.[25]

Regarding the backward peaked IO angular distribution of the $O(^1D)$ reaction (see Fig. 7(c) and Fig. 8 (top right)), this may arise from a direct process at small impact parameters for nearly collinear geometry on the singlet PES. About the possibility of singlet to triplet ISC, this is not expected to take place for collinear geometry because of the lack of curve crossing;[15] it could occur for bent geometry, but there is no direct evidence of it since the angular distribution is sharply peaked at $\theta = 180°$. The large fraction (50%) of energy released in translation reflects a strong repulsion among the fragments while they separate on the exit valley of the singlet PES. Direct backward scattering on the singlet PES, accompanied by a similarly large fraction of recoil energy, was also observed in CMB studies of the reactions $O(^1D) + HX \rightarrow XO + H$ (X = Cl, Br).[22,23] Notably, this backward feature was absent in $O(^1D) + HI$.[25] Recent quasiclassical trajectory calculations on an *ab initio* PES corroborate the experimental backward scattering micromechanism for $O(^1D) + HCl \rightarrow ClO + H$ and attribute it to side attachment of $O(^1D)$ to the Cl atom at small impact parameters.[57]

### Comparison with the reactions K + $CH_3I$ and F + $CH_3I$

It may be interesting to compare the dynamics of $O(^3P) + CH_3I$ with those of the well studied reactions of alkali and alkaline-earth atoms, and also of halogen atoms, with $CH_3I$.

The reactions of alkali atoms with methyl iodide have played a significant role in the development of reaction dynamics.[1] In particular, the exoergic reaction $K + CH_3I \rightarrow KI + CH_3$ ($\Delta H \approx -88$ kJ mol$^{-1}$) has been studied in CMB since the early days of the technique.[58] These systems have been benchmarks for the investigation of chemical stereodynamics: by orienting $CH_3I$ with an hexapole field it was shown that the reaction preferentially occurs when the alkali atom collides with the iodine end of the $CH_3I$ molecule.[59] More recently, the $K + CH_3I$ reaction was studied by using the brute force technique to control the $CH_3I$ approach geometry (stereodynamical control).[60] Strong backward scattering of KI (with respect to the K atom direction) was found both at low and high collision energies, and the results were rationalized in terms of the DIPR (direct impulse product repulsion) model,[1] if a 108° wide cone of acceptance centered around the collinear conformation K–I–$CH_3$ is assumed.[60] A tight correlation exists between the orientation of the axis of I–$CH_3$ and the scattering angle of the products in the c.m. system. The product recoil energy is very high (up to 60–70% of the maximum). The direct abstraction of iodine atoms by $O(^3P)$ from $CH_3I$ on the triplet PES exhibits very similar features to $K + CH_3I$, which witnesses similarities in the topology of the PESs involved.

The abstraction of I atoms from $CH_3I$ by F atoms is an exoergic reaction ($\Delta H \approx -45$ kJ mol$^{-1}$) with a mechanism involving a collision complex with a lifetime that depends on the collision energy.[61] A long-lived complex occurs at low $E_c$ ($\approx$11 kJ mol$^{-1}$), with about 30% of product recoil energy, while an osculating complex is occurring at high $E_c$ ($\approx$60 kJ mol$^{-1}$). This is due to the stability of the $CH_3IF$ complex by about 105 kJ mol$^{-1}$ with respect to the reagents. Notably, the product energy distribution in the reaction $F + CH_3I$ was shown to be fairly consistent with phase space statistical models. The formation of IO from the reactions of $O(^3P)$ *via* ISC, and also of $O(^1D)$, with $CH_3I$ proceeding *via* a long-lived/osculating complex on the singlet PES exhibits a reaction dynamics similar to that of F atoms with $CH_3I$. A common feature of these reactions is the existence of a bound complex intermediate along the minimum energy path of the PES.

## V. Conclusion

The reaction of atomic oxygen with $CH_3I$ to form $IO + CH_3$ proceeds with different mechanisms depending on the electronic state of the atom and of the geometry of the approach of the reactants. For nearly collinear geometry of approach, the $O(^3P)$ reaction proceeds on the triplet PES with rebound dynamics, similar to that exhibited by K atoms with $CH_3I$: both reactions exhibit a backward peaked angular distribution and a strong repulsive product energy release. However, in

the case of the O atom reaction, for bent geometry there is a significant probability of a non-adiabatic transition from the triplet to the singlet PES, which leads the reactants to experience the deep singlet well and, *via* formation of a long-lived complex intermediate, to IO + $CH_3$ formation with a backward/forward symmetric angular distribution and a much higher internal excitation of the products. These findings are corroborated by recent *ab initio* calculations on the O($^3$P,$^1$D) + $CH_3I$ system, which highlight the role of intersystem crossing for bent geometry[15] and are in line with the interpretation of previous CMB experiments on the similar reactions of O($^3$P) with larger alkyl and haloalkyl iodides.[27–33]

Electronic excitation of the oxygen atom to the ($^1$D) state drives the reaction with $CH_3I$ directly on the singlet PES. In this case both the addition and insertion complex are possible. Because of the much larger exoergicity with respect to the O($^3$P) reaction, the bound singlet complex lives only a time comparable to its rotational period and the IO angular distribution is forward peaked. Differences in the polarization of the product angular distributions as well as in the product recoil energy distribution between O($^1$D) + $CH_3I \rightarrow IO + CH_3$ and the similar reaction of O($^1$D) + HI → IO + H are due to differences in mass combination, and to the fact that $CH_3$ has internal degrees of freedom, and this is corroborated by phase space theory calculations. A second mechanism for O($^1$D) on the singlet PES, exhibits backward scattered product with large repulsive energy release and arises from small impact parameter collisions, which do not sample the potential well. This same micromechanism was also observed for O($^1$D) + HCl and HBr leading to ClO and BrO formation, while, notably, not for O($^1$D) + HI.

The dynamics of the O($^3$P) reaction *via* ISC and long-lived complex formation appears to be statistical, as shown by the very good agreement between the experimental product angular and translational energy distributions and the results of a phase space theory that imposes conservation of energy and angular momentum. In contrast, the dynamics of the O($^1$D) reaction proceeding through an osculating singlet complex is not fully statistical, indicating that complete energy randomization does not occur within one rotational period of the collision complex.

Support by the Italian "Consiglio Nazionale delle Ricerche" and "Ministero Università e Ricerca Scientifica", and the AFOSR (grant F617-08-94-C-0013) through EOARD (grant SPC-94-4042) is gratefully acknowledged.

## References

1 R. D. Levine and R. B. Bernstein, *Molecular Reaction Dynamics and Chemical Reactivity*, Oxford University Press, New York, 1987.
2 M. J. Bronikowski, W. R. Simpson and R. N. Zare, *J. Phys. Chem.*, 1993, **97**, 2194; *ibid.*, 1993, **97**, 2204; R. B. Metz, J. M. Pfeiffer, J. D. Thoemke and F. F. Crim, *Chem. Phys. Lett.*, 1994, **221**, 347.
3 J. M. Bowman and G. C. Schatz, *Annu. Rev. Phys. Chem.*, 1995, **46**, 169.
4 R. J. Donovan and D. Husain, *Chem. Rev.*, 1970, **70**, 489; K. Schofield, *J. Phys. Chem. Ref. Data*, 1979, **8**, 723.
5 G. C. Schatz, A. Papaioannou, L. A. Pederson, L. B. Harding, T-S. Ho, T. Hollebeek and H. Rabitz, *J. Chem. Phys.*, 1997, **107**, 2340.
6 R. Grice, *Acc. Chem. Res.*, 1981, **14**, 37.
7 See, for instance, A. B. McCoy, M. W. Lufaso, M. Veneziani, S. Atrill and R. Naaman, *J. Chem. Phys.*, 1998, **108**, 9651; A. J. Alexander, D. A. Blunt, M. Brouard, J. P. Simons, F. J. Aoiz, L. Banares, Y. Fujimura and M. Tsubouchi, *Faraday Discuss.*, 1997, **108**, 375; G. M. Sweeney, A. Watson and K. G. McKendrick, *J. Chem. Phys.*, 1997, **106**, 9172; R. Grice, *Int. Rev. Phys. Chem.*, 1995, **14**, 315; R. Zhang, W. J. Van den Zande, M. J. Bronikowski and R. N. Zare, *J. Chem. Phys.*, 1991, **94**, 2704; A. M. Schmoltner, P. M. Chu, R. J. Brudzynski and Y. T. Lee, *J. Chem. Phys.*, 1989, **91**, 6926; J. J. Sloan, *J. Phys. Chem.*, 1988, **92**, 18.
8 P. Casavecchia, N. Balucani and G. G. Volpi, in *Advanced Series in Physical Chemistry Vol. 6. The Chemical Dynamics and Kinetics of Small Radicals*, ed. A. Wagner and K. Liu, World Scientific, Singapore, 1995, p. 365; and references therein.
9 P. Casavecchia, N. Balucani and G. G. Volpi, in *Research in Chemical Kinetics*, ed. R. G. Compton and G. Hancock, Elsevier, Amsterdam, 1993, vol. 1, p. 1.
10 N. Balucani, L. Beneventi, P. Casavecchia, D. Stranges and G. G. Volpi, *J. Chem. Phys.*, 1991, **94**, 8611.
11 M. Alagia, N. Balucani, P. Casavecchia, D. Stranges and G. G. Volpi, *J. Chem. Soc., Faraday Trans.*, 1995, **91**, 575.
12 M. K. Gilles, A. A. Turnipseed, Y. Rudich, R. K. Talukdar, P. Villalta, L. G. Huey, L. B. Burkholder and A. R. Ravishankara, *J. Phys. Chem.*, 1996, **100**, 14005.

13 J. E. Thompson and A. R. Ravishankara, *Int. J. Chem. Kinet.*, 1993, **25**, 479; A. P. Force and J. R. Wiesenfeld, *J. Phys. Chem.*, 1981, **85**, 782; J. M. Cronkhite and P. H. Wine, *Int. J. Chem. Kinet.*, 1998, **30**, 555.
14 M. Hawkins and L. Andrews, *Inorg. Chem.*, 1985, **24**, 3285.
15 A. Misra, R. J. Berry and P. Marshall, *J. Phys. Chem.*, 1997, **101**, 7420.
16 W. L. Chameides and D. D. Davis, *J. Geophys. Res.*, 1980, **85**, 7383.
17 S. Solomon, R. R. Garcia and A. R. Ravishankara, *J. Geophys. Res.*, 1994, **99**, 20491.
18 S. Solomon, J. B. Burkholder, A. R. Ravishankara and R. R. Garcia, *J. Geophys. Res.*, 1994, **99**, 20929.
19 Yu. Bedjanian, G. Le Bras and G. Poulet, *J. Phys. Chem. A*, 1997, **101**, 4088; *ibid.*, 1998, **102**, 10501; A. A. Turnipseed, M. K. Gilles, L. B. Burkholder and A. R. Ravishankara, *J. Phys. Chem. A*, 1997, **101**, 5517.
20 F. Maguin, G. Laverdet, G. Le Bras and G. Poulet, *J. Phys. Chem.*, 1992, **96**, 1775.
21 B. Alicke, K. Hebestreit, U. Platt, L. J. Carpenter and W. T. Sturges, *Ann. Geophys.*, 1998, **16** (Suppl. II), C716.
22 N. Balucani, L. Beneventi, P. Casavecchia and G. G. Volpi, *Chem. Phys. Lett.*, 1991, **180**, 34.
23 N. Balucani, L. Beneventi, P. Casavecchia, G. G. Volpi, E. J. Kruus and J. J. Sloan, *Can. J. Chem.*, 1994, **72**, 888.
24 M. Alagia, N. Balucani, P. Casavecchia, A. Laganà, G. Ochoa de Aspuru, E. H. van Kleef, G. G. Volpi and G. Lendvay, *Chem. Phys. Lett.*, 1996, **258**, 323.
25 M. Alagia, N. Balucani, P. Casavecchia and G. G. Volpi, *J. Phys. Chem.*, 1997, **101**, 6455.
26 J. J. Rochford, L. J. Powell and R. Grice, *J. Phys. Chem.*, 1995, **99**, 13647; L. J. Powell, D. D. Wells, J. J. Wang, D. J. Smith and R. Grice, *Mol. Phys.*, 1996, **87**, 865.
27 J. J. Wang, D. J. Smith and R. Grice, *J. Phys. Chem.*, 1996, **100**, 6620.
28 J. J. Wang, D. J. Smith and R. Grice, *J. Phys. Chem. A*, 1997, **101**, 3293.
29 J. J. Wang, D. J. Smith and R. Grice, *J. Phys. Chem.*, 1996, **100**, 13603.
30 D. D. Wells, S. Mohr, K. M. Goonan, M. Hammer and R. Grice, *J. Phys. Chem. A*, 1997, **101**, 7499.
31 X. Gao, J. Essex-Lopresti, S. Munro, M. P. Hall, D. J. Smith and R. Grice, *J. Chem. Soc., Faraday Trans.*, 1997, **93**, 4119.
32 X. Gao, J. Essex-Lopresti, S. Munro, D. J. Smith and R. Grice, *J. Phys. Chem. A*, 1998, **102**, 1912.
33 R. Grice, *Int. Rev. Phys. Chem.*, 1995, **14**, 315.
34 P. Casavecchia, *Sci. Spectra*, 1996, **6**, 56.
35 S. J. Sibener, R. J. Buss, C. Y. Ng and Y. T. Lee, *Rev. Sci. Instrum.*, 1980, **51**, 167.
36 M. Alagia, V. Aquilanti, D. Ascenzi, N. Balucani, D. Cappelletti, L. Cartechini, P. Casavecchia, F. Pirani, G. Sanchini and G. G. Volpi, *Isr. J. Chem.*, 1997, **37**, 329.
37 K. Sköld, *Nucl. Instrum. Methods*, 1968, **63**, 114.
38 Y. T. Lee, in *Atomic and Molecular Beam Methods*, ed. G. Scoles, Oxford University Press, New York, 1987, vol. 1; T. T. Warnock and R. B. Bernstein, *J. Chem. Phys.*, 1968, **49**, 1878.
39 R. W. P. White, D. J. Smith and R. Grice, *J. Phys. Chem.*, 1993, **97**, 2123.
40 R. A. Marcus, *J. Chem. Phys.*, 1965, **43**, 2658.
41 M. W. Chase, *J. Phys. Chem. Ref. Data*, 1996, **25**, 1297, and references therein.
42 D. Radlein, J. C. Whitehead and R. Grice, *Nature* (*London*), 1975, **253**, 5486.
43 R. J. Buss, S. J. Sibener and Y. T. Lee, *J. Phys. Chem.*, 1983, **87**, 4840.
44 M. P. McGrath and F. S. Rowland, *J. Phys. Chem.*, 1996, **100**, 4815.
45 Y. Bedjanian, G. Le Bras and G. Poulet, *J. Phys. Chem.*, 1996, **100**, 15130.
46 G. A. Fisk, J. D. McDonald and D. R. Herschbach, *Discuss. Faraday Soc.*, 1967, **44**, 228.
47 J. C. Light, *J. Chem. Phys.* 1964, **40**, 3221; P. Pechukas and J. C. Light, *J. Chem. Phys.*, 1965, **42**, 3281; E. E. Nikitin, *Theory of elementary atomic and molecular processes in gases*, Clarendon Press, Oxford, 1974, Sect. 28–31 and 50; C. E. Klots, *Z. Naturforsch. A: Phys. Chem. Kosmoṕhys.*, 1972, **27**, 553; R. A. Marcus, *J. Chem. Phys.*, 1975, **62**, 1372; P. J. Dagdigian, H. W. Cruse, A. Schultz and R. N. Zare, *J. Chem. Phys.*, 1974, **61**, 4450; W. J. Chesnavitch and M. T. Bowers, *J. Chem. Phys.*, 1977, **66**, 2306; L. Bonnet and J. C. Rayez, *Chem. Phys.*, 1995, **201**, 203.
48 L. Bonnet and J. C. Rayez, *Phys. Chem. Chem. Phys.*, 1999, **1**, 2383.
49 D. M. Wardlaw and R. A. Marcus, *Adv. Chem. Phys.*, 1988, **70**, 231.
50 I. W. M. Smith, *J. Chem. Educ.*, 1982, **59**, 9; R. D. Levine and R. B. Bernstein, *Chem. Phys. Lett.*, 1984, **105**, 467.
51 L. Bonnet, J. C. Rayez and P. Casavecchia, to be published.
52 R. A. Loomis, J. J. Klaassen, J. Lindner, P. G. Christopher and S. R. Leone, *J. Chem. Phys.*, 1997, **106**, 3934; R. A. Loomis, S. R. Leone and M. K. Gilles, *Res. Chem. Intermed.*, 1998, **24**, 707.
53 J. E. Stevens, Q. Cui and K. Morokuma, *J. Chem. Phys.*, 1998, **108**, 1544.
54 Y. Matsumi and S. M. Shamsuddin, *J. Chem. Phys.*, 1995, **103**, 4490.
55 D. R. Herschbach, *Adv. Chem. Phys.*, 1966, **10**, 319; *Faraday Discuss. Chem. Soc.*, 1973, **55**, 233.
56 L. Bonnet and J. C. Rayez, *J. Phys. Chem. A*, 1998, **102**, 3455.
57 J. M. Alvariño, A. Rodriguez, M. L. Hernandez and A. Laganà, *Chem. Phys. Lett.*, in the press.
58 D. R. Herschbach, G. H. Kwei and J. A. Norris, *J. Chem. Phys.*, 1961, **34**, 1842; *ibid.*, 1970, **52**, 1317; A. M. Rulis and R. B. Bernstein, *J. Chem. Phys.*, 1972, **57**, 5497.
59 P. R. Brooks and E. M. Jones, *J. Chem. Phys.*, 1966, **45**, 3449; R. J. Beuhler, R. B. Bernstein and K. H.

Kramer, *J. Am. Chem. Soc.*, 1966, **88**, 5331; D. H. Parker and R. B. Bernstein, *Annu. Rev. Phys. Chem.*, 1989, **40**, 561.
60 H. J. Loesch and A. Remscheid, *J. Phys. Chem.*, 1991, **95**, 8194; H. J. Loesch, *Annu. Rev. Phys. Chem.*, 1995, **46**, 555.
61 J. M. Farrar and Y. T. Lee, *J. Chem. Phys.*, 1975, **63**, 3639.

*Paper 9/02949D*